2.3 Separation of low viscosity crude oil and brine signal

In systems where bulk brine is present, as in double emulsion; water droplets confined in oil droplets confined in a bulk water phase, or low viscosity oils where T_2 overlap with the T_2*'s* of the brine due to comparable viscosity, we have designed the following approach for measuring the *DSD*: As the root of the mean squared displacement (*X*) of the water confined in droplets is limited by the droplet size ($X_{DSD} \leq$ *droplet radius*), the observation time in the convection compensated sequence in figure 3.1 is made so long that $X_{DSD} << X_{bulk}$, $X_{low\ viscosity\ oil}$. For example with Δ of 1 second the *X* of water at 25°C would be ~100µm. This will be much larger than the typical droplet diameter we report to be measured here, ~ (1-20) µm
In figure 2.2 it is shown how one may resolve the signal from the water inside the droplets from the water and/or low viscosity oil that move more freely. When the observation time is made so short that X_{bulk} , $X_{low\ viscosity\ oil} \approx X_{DSD}$, we will have a situation where we are not able to resolve the water confined in droplets from the bulk water or the low viscosity oil ('•' in figure 2.2), but as we increase the observation time we eventually arrive at the situation where $X_{DSD} << X_{bulk}$, $X_{low\ viscosity\ oil}$ ('+' in figure 2.2). Then we may easily resolve the water confined in droplets and measure the average squared droplet radius according to equation 2.3.

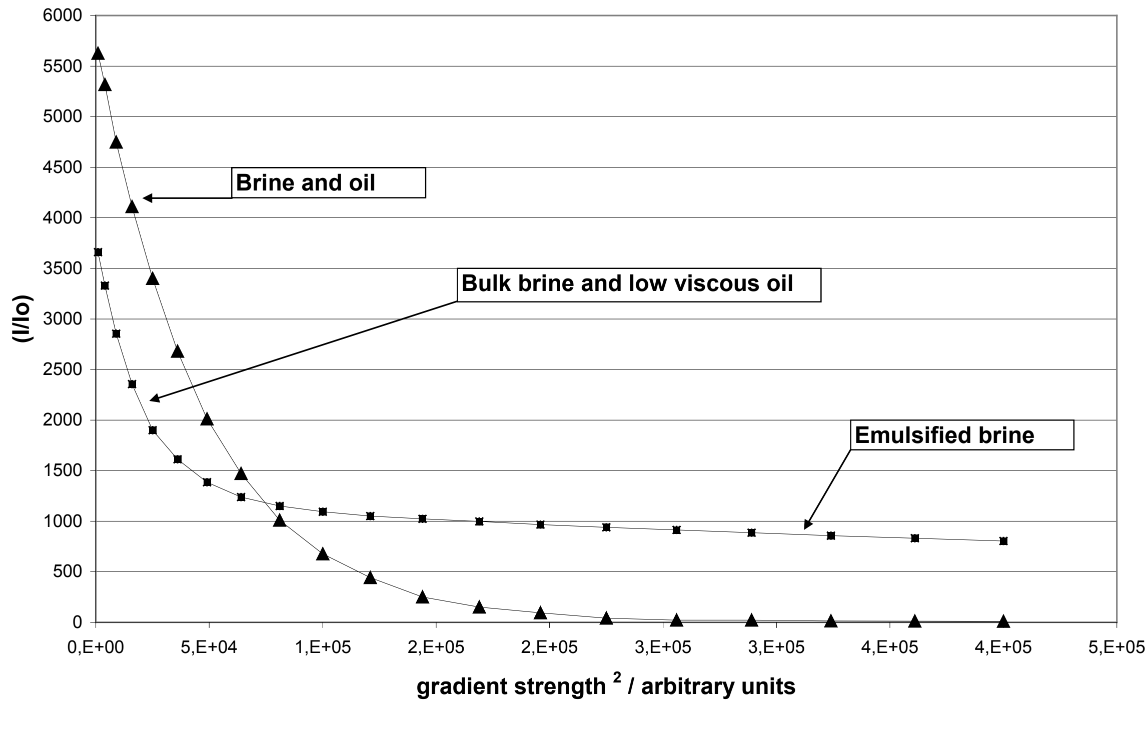

Figure 2.2: Resolving emulsified brine by increasing the observation time from short (▲) to long (■).

3. Experimental

3.1 The NMR experiments

The NMR experiments were performed on a 21 MHz benchtop NMR system supplied by Anvendt Teknologi AS and Advanced Magnetic Resonance. The gradient system has the ability of delivering approximately 400 G/cm at full power.

In figures 3.1-3.2 we have shown the sequences for suppressing bulk water and or the oil (regardless of viscosity), measuring the average squared droplet radius and the T_2 attenuation of the water confined in the droplets of the emulsion. The applied gradient pulse length used was 800 μs and the τ-value in the 13-interval sequence was 1.5 ms.

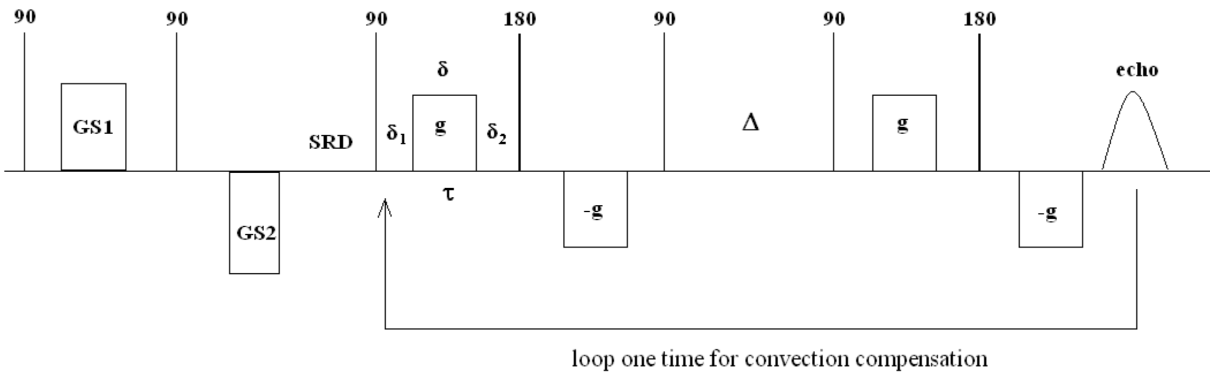

Figure 3.1. The combined spoiler recovery - 13 interval PFGSTE sequence with convection compensation

The corresponding attenuations for the sequence in figure 3.1 is written

$$I = I_0 e^{-2(\gamma^2 \delta^2 g^2 D_{(\Delta)} (\Delta + \frac{3\tau}{2} - \frac{\delta}{6}))} e^{-2(\frac{\Delta}{T_1} + \frac{4\tau}{T_2})} \qquad (3.1)$$

where I_0 is the initial NMR signal intensity, γ is the gyromagnetic ratio, δ is the gradient pulse length, g is the strength of the gradient of the applied pulsed magnetic field, $D(\Delta)$ is the molecular diffusion coefficient, Δ is the z-storage delay, T_1 is the longitudinal relaxation time, T_2 is the transverse relaxation time and 2τ is the inter echo spacing.

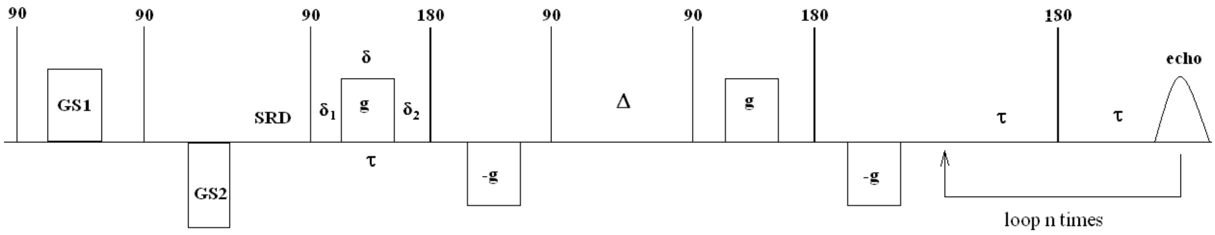

Figure 3.2. The combined spoiler recovery - 13 interval PFGSTE - CPMG sequence

The corresponding attenuations for the sequence in figure 3.1 is written

$$I = I_0 e^{-(\gamma^2\delta^2 g^2 D_{(\Delta)}(\Delta+\frac{3\tau}{2}-\frac{\delta}{6}))} e^{-(\frac{\Delta}{T_1}+\frac{2n\tau}{T_2})} \qquad (3.2)$$

where n is the echo number. The tool for performing a one dimensional inverse Laplace transform on the CPMG data was supplied by Anvendt Teknologi AS.

3.2 Preparation of Emulsions

The emulsions containing high viscosity oil were prepared by mixing the crude oils with water at room temperature (22°C), the total sample volume being 20 ml. As a mixer we applied an Ultra Turrax (Ika®–Werke Co., Germany) homogenizer (18 mm head) with a stirring speed of 20 000 rpm for 2 minutes. The emulsions with water cut of 30% were analyzed immediately after mixing.

The emulsion containing low viscosity oil was prepared by mixing the oil and water phases at the ambient temperature (22°C ± 1°C). The total volume of the emulsion was 10 ml and aqueous phase volume fraction of the emulsion was 0.30. 3 ml of Milli-Q water containing 3.5% NaCl and 7 mL of decane containing 2% (w/v) sorbiton sesquioleate (SPAN 83) were put into 25 ml glass tube and then mixed with Ultra Turrax (Ika®–Werke Co., Germany) using T25 with a 10 mm head at 24 000 rpm for 3 minutes. After the emulsification, the emulsions were correspondingly analyzed both with NMR and microscope.

3.3 Droplet Size Distribution Measured by Microscope

A Nikon Eclipse ME 600 digital video microscope with Image Pro Plus 5.0 software from Media Cybernetics and a CoolSNAP-Pro cfw 4 megapixel cooled CCD camera was used to determine droplet size distribution of the emulsion. The microscope contains the lens with the CFI LU Plan Epi 10 X with an numerical aperture of 0.30 and is capable of measuring the droplet size down to about 1 µm. Droplet size distribution of the emulsion was determined applying the following procedure: first the emulsion was diluted in the oil (1/20 (v/v)), because the original emulsion was too concentrated to separate and distinguish the droplets using the microscope, and 1–2 drop of the diluted emulsion placed on a glass slide. Afterward, the diluted emulsion was placed under the microscope and then several pictures were optimized and captured. The clusters and non-droplets were removed from the captured pictures and then the droplets were counted and the diameters were calculated using the Image Pro Plus 5.10 software. To obtain the distribution population of the droplets in the emulsion more than 300 droplets were chosen from the captured pictures and then analyzed.

4. Results and discussion

4.1 Droplet size distribution from a system containing high viscosity oil

One of the important features of the proposed method is that we are able to suppress the oil signal in two different ways, either by using a long observation time Δ, which is applicable for high viscosity oil samples and/or by applying strong enough magnetic pulsed field gradients in the 13 interval PFGSTE sequence, which is applicable for low viscosity oils. For oils with intermediate viscosity both effects will contribute to resolve the signal from water confined in the droplets from the oil signal.

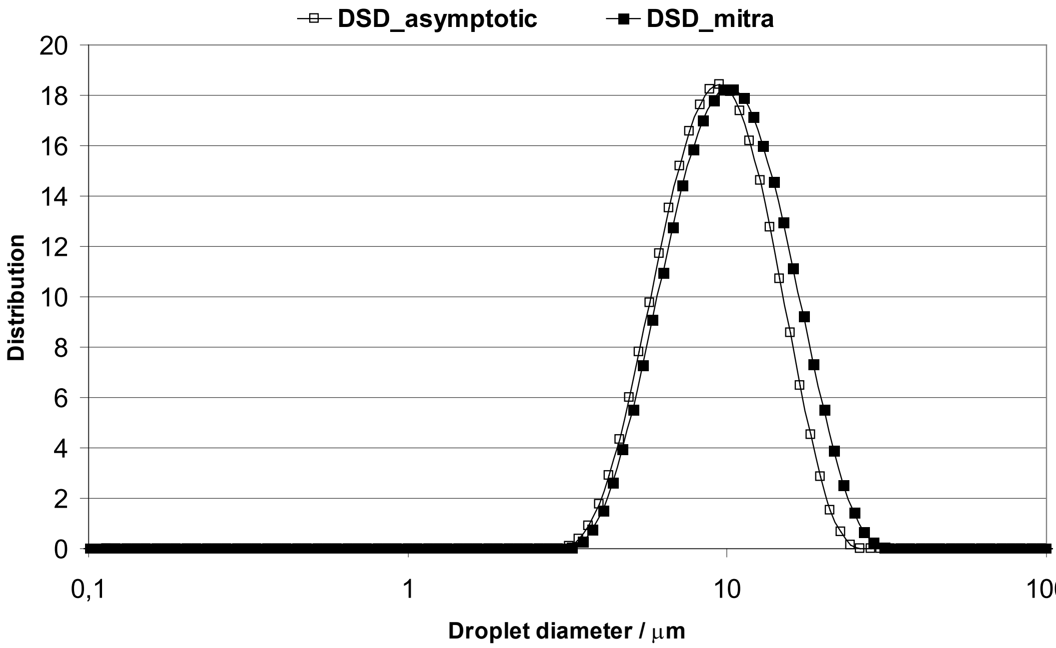

Figure 4.1: Comparison of the proposed method (*DSD_asymptotic*) against the method developed by Opedal et.al (*DSD_mitra*)

In figure 4.1 we have compared the method proposed here (*DSD_asymptotic*) against the method developed by Opedal et.al [15]. The system investigated was brine in crude oil emulsion with 30 % brine content/water cut, the very same as measured on by Opedal et.al [15]. The T_1's of the crude oil were situated around 200 ms, so we could easily suppress the oil signal by using a Δ of 500 ms (i.e. 2Δ=1 second). The two droplet size distributions (*DSD*) are almost identical, and it confirms that both methods do measure the DSD quite accurately (*DSD_mitra* has already been validated against microscopy [15].

4.2 Droplet size distribution from a system containing high viscosity oil

In figure 4.2 we show the results from an emulsion containing decane as the oil phase. In the bulk phase the decane is of practically the same viscosity as the bulk phase of the brine. Thus T_1 and T_2*'s* are overlapping, and we must combine relatively long Δ with magnetic field gradients to resolve the signal of the brine confined in the droplets ('■' in figure 2.2). The Δ used was 35 ms, but as the droplets were quite small, this observation time was sufficient to reach the asymptotic limit as given by Packer et.al (equation 2.1). When comparing with microscopy we do find a reasonable agreement between the two methods. The *DSD* from the NMR method seems to be more broadened, but to get a sharper distribution from NMR it is just a matter of choosing the smoothing parameter in the inverse Laplace routine differently. However, as the microscopy arises from the counting of 306 droplets only and considering the fact that the droplet diameters are close to the resolution limit of the microscope, it is likely that the true *DSD* is broadened as shown by the NMR result. Most important is that the average droplet diameter from the two number based distributions are found to be quite similar, 1.5 μm from microscopy versus 1.8 μm from NMR.

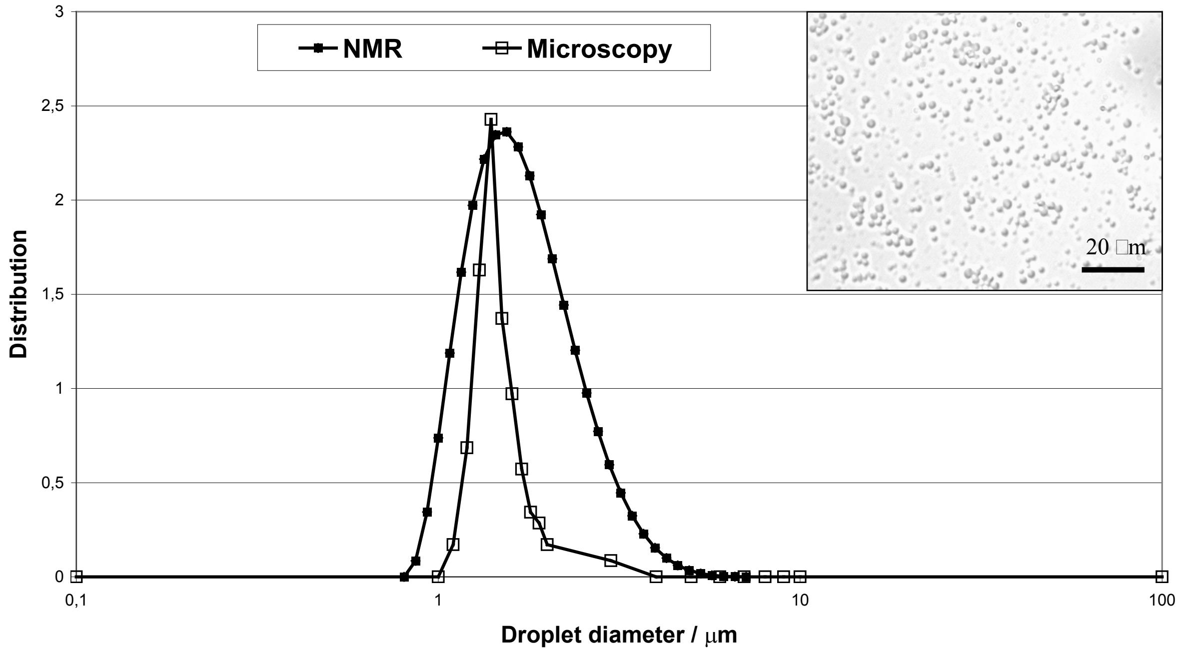

Figure 4.2 Comparison between *DSD_asymptotic* ('+') and microscopy ('□')

4.3 On the use of the NMR method for measuring DSD in a brine in oil emulsion containing low viscosity oil phase.

When measuring the brine in decane system we realized that there was a strong Δ dependency on the measured *DSD*. As the sequence used was a convection compensated sequence, it was not likely to arise from sedimentation of the droplets, but more a brownian movement of the droplets themselves. As the droplets turned out to be quite small, the thermal movement of the droplets is likely to appear when they are confined in low viscosity oil as decane.

In figure 4.3 we plot the average droplet diameter for the two emulsion systems investigated as a function of the square root of Δ. The emulsion system containing the low viscosity oil exhibit a strong dependency of Δ down to approximately 50 ms, then it levels out. Measurements below 25 ms are not conducted as one then is leaving the regime where the asymptotic approach is valid ($X_{DSD} << X_{bulk}$), i.e the apparent measured droplet diameter starts to increase. Therefore care must be taken when choosing Δ for determining the average squared droplet radius, and it is probably wise to check for several Δ-values. Indeed, if brine droplets were allowed to move freely one would expect a linear dependency of measured root of the mean squared displacement, but in figure it reaches a plateau value. This is probably due to the fact that the system measured on had water cut of 60% and it continued to sediment until it had a closed sphere packing of 70% brine droplets. Thus the picture of brownian movement only does not fit to the system. The impact of the packing of the spheres must be taken into account, but is addressed further here.

We also see a small dependency of Δ on the emulsion with high viscosity oil. However this is not due to movement of the droplet, but more likely an effect of a finite width of the relaxation times. The measured droplet diameter is fairly constant up to Δ≈0.5 seconds but then starts to increase slightly. As the T_1 relaxation times of the brine phase is centred around 1 second, the average droplet diameter will be biased towards the larger droplets with the largest T_1 values, and this is exactly what we seen in figure 4.3. As Δ passes 1 second the measured average droplet diameter increases

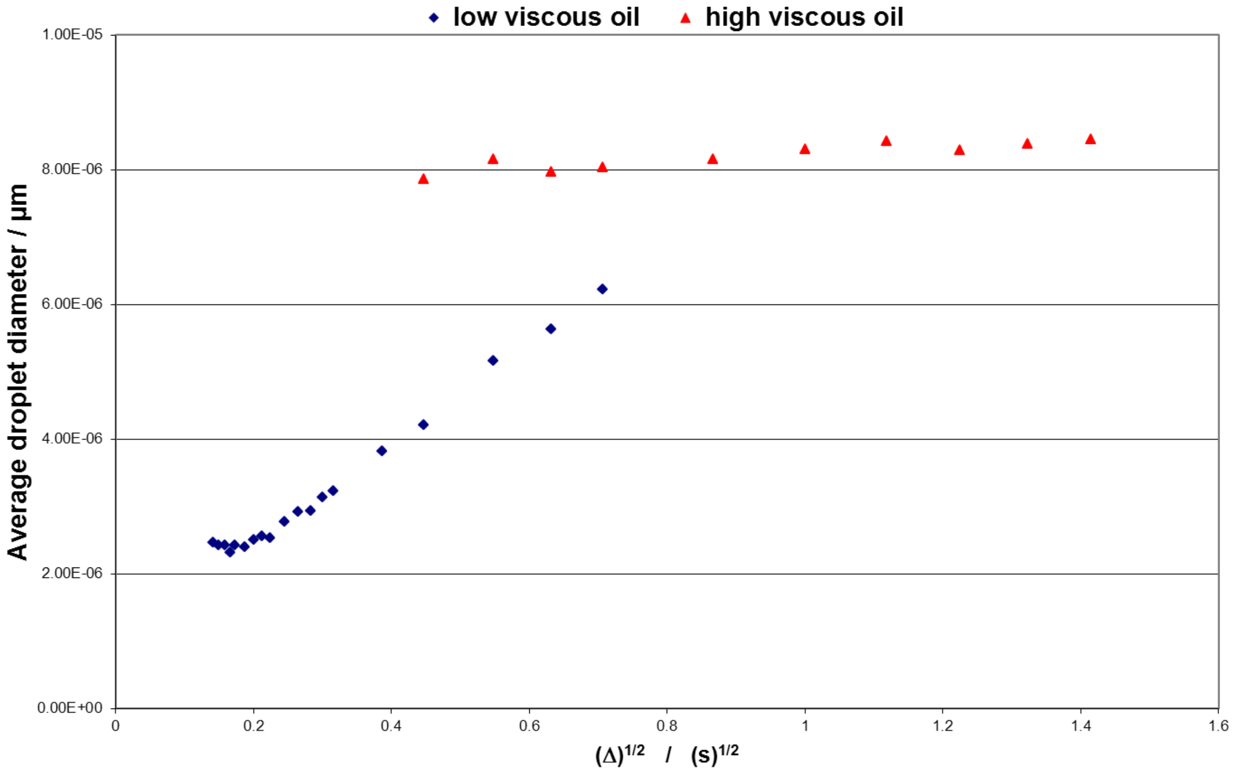

Figure 4.3: Measured volume average droplet radius as a function of observation time Δ

Finally, one should ask what if the droplets were so large that the asymptotic limit (eq. 2.1) was not valid and the movement of the droplets kept us away from reaching the plateau region as shown in figure 4.3? In such a situation it would probably be better to apply the Mitra approach instead [15, 24], but then with a 13 interval PFGSTE sequences in front that is used to suppress low viscosity oil and bulk water. Work is in progress to develop such a method/procedure.

5. Conclusion

A method for fast determination of droplet size distribution of water in oil emulsions is presented, and it returns distributions that are in good agreement with the expected droplet size distribution regardless of the oil viscosity.

References

[1] Tanner, J.E. and E.O. Stejskal, The Journal of Chemical Physics, 1965: p. 288-292.

[2] Tanner, J.E. and E.O. Stejskal, The Journal of Chemical Physics, 1968. 49: p. 1768-1777.

[3] Goudappel, G.-J.W., J.P.M.v. Duynhoven, and M.M.W. Mooren, Journal of Colloid and Interface Science, 2001. 239: p. 535-542.

[4] Fourel, I., J.P. Guillement, and D.L. Botlan, Journal of Colloid and Interface Science, 1995. 169: p. 119-124.

[5] Duynhoven, J.P.M.v., et al., European Journal of Lipid Science and Technology 2007. 109: p. 1095-1103.

[6] Kiokias, S., A.A. Reszka, and A. Bot, International Dairy Journal, 2004. 14: p. 287-295.

[7] Aichele, C.P., et al., Journal of Colloid and Interface Science, 2007. 315: p. 607-619.

[8] Packer, K.J. and C. Rees, Journal of Colloid and Interface Science, 1972. 40(2): p. 206-218.

[9] Li, X., J.C. Cox, and R.W. Flumerfelt, The American Institute of Chemical Engineers Journal, 1992. 38(10): p. 1671-1674.

[10] Balinov, B., O. Söderman, and T. Wärnheim, Journal of the American oil Chemists' Society, 1994. 71(5): p. 513-518.

[11] Enden, J.C.v.d., et al., Journal of Colloid and interface Science, 1990. 140(1): p. 105-113.

[12] Callaghan, P.T., K.W. Jolley, and R.S. Humphrey, Journal of Colloid and Interface Science, 1983. 93(2): p. 521-529.

[13] Peña, A.A. and G.J. Hirasaki, Advances in Colloid and Interface Science, 2003. 105: p. 103-150.

[14] R. Bernewitz, G. Guthausen, and H. P. Schuchmann, Magnetic Resonance in Chemistry, 2011. 49: p 93-104

[15] N. van der Tuuk Opedal, G.H.Sørland, and Johan Sjöblom, Diffusion Fundamentals 9, 2009, pp 1-29

[16] G.H. Sørland, AIP Conference Proceedings Vol. 1330, 2011, p 27-31

[17] G. H. Sørland, H. W. Anthonsen, K. Zick, J. Sjöblom, and S. Simon, Diffusion Fundamentals 2011, pages 1-9

[18] H. W. Anthonsen, G. H. Sørland, K. Zick, J. Sjöblom, and S. Simon, Diffusion Fundamentals 2012, pages: 1-12

[19] Kärger, J. and D.M. Ruthven, Diffusion in Zeolites and other Microporous Solids. 1992, New York: Wiley.

[20] Balinov, B. and O. Söderman, Emulsion - the NMR Perspective. Encyclopedic Handbook of Emulsion Technology, ed. J. Sjöblom. 2001, New York: Marcel Dekker.

[21] Cohen, M.H. and K.S. Mendelson, Journal of Applied Physics, 1982. 53: p. 1127

[22] Uh, J. and A.T. Watson, Industrial & Engineering chemistry research, 2004. 43: p. 3026-3032.

[23] S.W. Provencher Comput. Phys. Commun. 27, (1982), 229–242.

[24] Mitra, P.P., P.N. Sen, and L.M. Schwartz, Physical Review B, 1993. 47(14): p. 8565-8574.